

## Heavy Petroleum Composition. 2. Progression of the Boduszynski Model to the Limit of Distillation by Ultrahigh-Resolution FT-ICR Mass Spectrometry

Amy M. McKenna,<sup>†</sup> Gregory T. Blakney,<sup>‡</sup> Feng Xian,<sup>†</sup> Paul B. Glaser,<sup>§</sup> Ryan P. Rodgers,<sup>\*,†,‡</sup> and Alan G. Marshall<sup>\*,†,‡</sup>

<sup>†</sup>Department of Chemistry and Biochemistry, Florida State University, 95 Chieftain Way, Tallahassee, Florida 32306,

<sup>‡</sup>National High Magnetic Field Laboratory, Florida State University, 1800 East Paul Dirac Drive, Tallahassee, Florida 32310-4005, and <sup>§</sup>General Electric Global Research, 1 Research Circle, Niskayuna, New York 12309-1027

Received February 5, 2010. Revised Manuscript Received April 18, 2010

Heavy petroleum fractions are structurally and compositionally complex mixtures that defy characterization by many traditional analytical techniques. Here, we present the detailed characterization of a Middle Eastern heavy crude oil distillation series, in further support of the Boduszynski model, which proposes that petroleum is a continuum with regard to composition, molecular weight, aromaticity, and heteroatom content as a function of the boiling point. Fourier transform ion cyclotron resonance mass spectrometry (FT-ICR MS) provides ultrahigh resolving power and mass accuracy and thereby allows for elemental assignment for each of the tens of thousands of peaks in a single crude oil sample. Part 1 of our five-part series established the validity of the Boduszynski model for the heavy vacuum gas oil (HVGO) distillation series. Here, we extend our analysis to fractions from a Middle Eastern heavy crude with cut temperatures including and *beyond* the middle distillate range. Collectively, the detailed compositional results for all heteroatom classes strongly support the continuity model. Interestingly, extrapolation of distillable compositional space to a high carbon number (up to 1 MDa) cannot account for the bulk properties of nondistillable (asphaltenic) species. Thus, either the continuity model does not accurately describe nondistillable petroleum materials (they are discontinuous in compositional space) or they are not high-molecular-weight (> 2000 Da) materials.

### Introduction

Understanding the boiling ranges of refinery feeds and products assists petroleum companies in strategy development and helps to predict the economic impact of a particular crude prior to production. Heavy crude oil is defined as crude with a high density (API gravity of 10°–20°) and high aromaticity, because of increased hydrogen deficiency.<sup>1</sup> For crude oil, the total content of solely hydrocarbon compounds ranges from >90% (by weight) for a light petroleum to 50% (by weight) for heavy crude oil.<sup>2</sup> Compounds containing heteroatoms (such as nitrogen, oxygen, sulfur, and metals such as vanadium, nickel, and iron) are present throughout the entire boiling range of crude oil, but increase in abundance in higher-boiling and nondistillable fractions.<sup>3</sup> Heteroatom-containing compounds, especially polar molecules, are responsible for difficulties in the refining, transportation, storage, and deposit formation of petroleum, and also concentrate in heavy, high-viscosity crudes.<sup>1,4</sup>

Although the *total* carbon and hydrogen content remains approximately constant (~83%–87% carbon and 11%–14%

hydrogen (by weight) across whole crudes of varying density) for light and heavy crudes, the hydrogen-to-carbon ratio (H/C) is significantly lower in the more-aromatic, higher-boiling fractions and resids, which are dominated by polynuclear aromatics, (e.g., multi-ring cycloalkane, aromatic, and polyaromatic structures) with minimal alkyl branching, and are less reactive than molecules with higher H/C ratios.<sup>2,3</sup> Because refineries work with increasingly challenging feedstocks, such as bitumen and heavy crude, comprehensive compositional characterization is paramount for the optimization of processes to increase the H/C ratio of products and facilitate the conversion of heavy ends into higher-value products.<sup>2</sup>

The analytical techniques routinely used for lighter feedstocks are inadequate for the characterization of heavy crudes and high-boiling materials. Low-boiling fractions, such as light and heavy naphtha (initial boiling point 220 °C) are amenable to gas chromatography (GC) or GC/MS for detailed compositional analysis, but not higher boiling feeds, because of low volatility and compositional complexity.<sup>4,5</sup> Even for middle distillate (kerosene and diesel) fractions (220–345 °C boiling range), GC/MS analysis suffers from insufficient resolution and nondefinitive data interpretation.<sup>6</sup> The advent of two-dimensional GC (GC × GC)<sup>7</sup> and high-temperature GC<sup>8</sup> has enabled detailed characterization of branched and normal

\*Authors to whom correspondence should be addressed. Tel.: +1 850 644 0529 (AGM), +1 850 644 2398 (RPR). Fax: +1 850 644 1366. E-mail addresses: marshall@magnet.fsu.edu (AGM), rogers@magnet.fsu.edu (RPR).

(1) Boduszynski, M. M. *Energy Fuels* **1987**, *1*, 2–11.  
(2) Speight, J. G. *Handbook of Petroleum Analysis*; Wiley Interscience: New York, 2001; Vol. 158.  
(3) Topsoe, H.; Bjerne, C. S.; Massoth, F. E. *Hydrotreating Catalysis: Science and Technology*; Springer-Verlag: New York, 1996; Vol. 11.  
(4) Betancourt, S. S.; Ventura, G. T.; Pomerantz, A. E.; Vilorio, O.; Dubost, F. X.; Zuo, J.; Monson, G.; Bustamante, D.; Purcell, J. M.; Nelson, R. K.; Rodgers, R. P.; Reddy, C. M.; Marshall, A. G.; Mullins, O. C. *Energy Fuels* **2009**.

(5) Mullins, O. C.; Martinez-Haya, B.; Marshall, A. G. *Energy Fuels* **2008**, *22*, 1765–1773.

(6) Bauserman, J. W.; Mushrush, G. W.; Hardy, D. R. *Ind. Eng. Chem. Res.* **2008**, *47*, 2867–2875.

(7) Reddy, C. M.; Nelson, R. K.; Sylva, S. P.; Xu, L.; Peacock, E. A.; Raghuraman, B.; Mullins, O. C. *J. Chromatogr., A* **2007**, *1148*, 100–107.

(8) Roehner, R. M.; Fletcher, J. V.; Hanson, F. V.; Dahdah, N. F. *Energy Fuels* **2002**, *16*, 211–217.

alkanes, alkylcyclopentanes, alkylcyclohexanes, and alkyl aromatics, but it is still unable to fully resolve heavy, high-boiling species. Comprehensive GC × GC increases the resolving power of traditional GC by subjecting each analyte to two different stationary phases with different chromatographic properties,<sup>9,10</sup> and, when coupled to various detectors, has found widespread use for hydrocarbon characterization of middle distillates, whose final boiling points are compatible with the maximum achievable GC analysis temperature.<sup>7,11–13</sup> However, for the characterization of higher-boiling residues (> 540 °C), extensive separation is necessary prior to most analytical techniques, including GC, GC × GC, and high-performance liquid chromatography (HPLC).

Boduszynski et al. conducted a comprehensive study of heavy oil composition and characterized heavy crude oil as a function of increasing boiling point, and they concluded that crude oil composition increased gradually and continuously with regard to aromaticity, molecular weight, and heteroatom content, and provided the first detailed compositional analysis of heavy petroleum fractions.<sup>1,14–17</sup> Complementary separation techniques coupled with mass spectrometry predicted the molecular nature of heavy crude oil. The authors concluded that “...compositional trends in fractions of increasing boiling point are continuous” and that “this continuity extends even to nondistillable residues”.<sup>14</sup> The atmospheric equivalent boiling point (AEBP), calculated from molecular weight and density or H/C ratio, characterized the boiling point range for distillable species and importantly postulated its extension to nondistillable residues.<sup>14,15</sup> That “continuity concept” states that crude oil compositional complexity and AEBP both increase smoothly and monotonically from light, low-boiling species to the most complex, highest-boiling fractions of crude oil.<sup>14</sup> A plot of molecular mass vs AEBP allows for comparison of different crude oils on a common basis with an emphasis on the importance of boiling range to selection of analytical technique for characterization.<sup>14</sup> The correlation between molar mass, heteroatom type, and boiling point is observed across the entire boiling range of petroleum products. Therefore, compositional trends for problematic, heavier fractions may be extrapolated from results obtained for lighter distillates.<sup>14</sup> The “continuity concept” of the Boduszynski model postulates that crude oil exhibits a continuous distribution in molecular weight, structure, and functionality from low boiling fractions to the nondistillable residues. However, validating that model requires complete molecular characterization of crude oil, which in turn requires a single analytical technique capable of addressing the challenges associated with complex crude oil mixtures. Although few techniques can handle the complexity associated with higher boiling fractions directly, ultrahigh-resolution mass spectrometry can

definitively determine heavy oil composition as a function of boiling point.

Boduszynski proposed a model applicable to *all* crudes based on one fundamental hypothesis: crude oil consists of relatively small molecules, with ~95% of the species lower than 2 kDa in size. Boduszynski postulated that the compositional trends observed for low and middle petroleum distillates continue into higher-boiling species, following the continuum to the limit of distillation, based on field-ionization mass spectrometry. Qian et al. used field desorption ionization mass spectrometry (FD MS) to characterize the molecular weight distributions of heavy petroleum fractions, and they outlined the continuity of molecular weight as a function of boiling point.<sup>18</sup> However, FD MS can create high-molecular-weight species through gas-phase reactions and produce erroneously high molecular weights.<sup>19,20</sup>

Fourier transform ion cyclotron resonance mass spectrometry (FT-ICR MS)<sup>21</sup> enables complex mixture analysis without prior separation. Compared with other mass spectrometry techniques, FT-ICR MS is unparalleled in its ability to characterize crude oil at the molecular level. The ultrahigh resolving power ( $m/\Delta m_{50\%} > 400\,000$ , in which  $\Delta m_{50\%}$  is the magnitude-mode mass spectral peak full width at half-maximum peak height) and the sub-ppm mass accuracy (< 400 ppb rms error) of FT-ICR MS allow for baseline resolution of closely spaced isobaric species and unambiguous molecular formula assignment of the tens of thousands of species present in a single mass spectrum of crude oil.<sup>22–25</sup>

Part I of this series validated the Boduszynski model for middle distillates from an HVGO distillation series of Athabasca bitumen, and provided the first comprehensive support of the Boduszynski model.<sup>26</sup> Here, we report atmospheric pressure photoionization (APPI) FT-ICR MS analysis of a Middle Eastern heavy crude oil distillation series to extend the Boduszynski model to the limit of distillation. Observed changes in molecular weight, heteroatom content, and aromaticity (reflected by double bond equivalents (DBE, defined as the number of rings plus double bonds)) as a function of the boiling point further validate the accuracy of the Boduszynski model and provide further testament to the relatively low molecular weight of heavy crude oil constituents.

## Experimental Methods

**Sample Preparation.** Solvents were HPLC grade (Sigma–Aldrich Chemical Co., St. Louis, MO). A Middle Eastern heavy crude was fractionated in two stages. Three fractions were generated from the initial distillation by use of a traditional

(9) Dalluge, J.; Beens, J.; Brinkman, U. A. *J. Chromatogr., A* **2003**, *1000*, 69–108.

(10) Frysinger, G. S.; Gaines, R. B.; Reddy, C. M. *Environ. Forensics* **2002**, *3*, 27–34.

(11) Vendeuvre, C.; Ruiz-Guerrero, R.; Bertocini, F.; Duval, L.; Thiebaut, D.; Hennion, M. C. *J. Chromatogr., A* **2005**, *1086*, 21–28.

(12) Mullins, O. C.; Ventura, G. T.; Nelson, R. K.; Betancourt, S. S.; Raghuraman, B.; Reddy, C. M. *Energy Fuels* **2008**, *22*, 496–503.

(13) Frysinger, G. S.; Gaines, R. B.; Xu, L.; Reddy, C. M. *Environ. Sci. Technol.* **2003**, *37*, 1653–1662.

(14) Boduszynski, M. M.; Altgelt, K. H. *Composition and Analysis of Heavy Petroleum Fractions*; CRC Press: New York, NY, 1994.

(15) Boduszynski, M. M.; Altgelt, K. H. *Energy Fuels* **1992**, *6* (1), 68–72.

(16) Boduszynski, M. M.; Altgelt, K. H. *Energy Fuels* **1992**, *6* (1), 72–76.

(17) Boduszynski, M. M. *Energy Fuels* **1988**, *2* (5), 597–613.

(18) Qian, K.; Edwards, K. E.; Siskin, M.; Olmstead, W. N.; Mennito, A. S.; Dechert, G. J.; Hoosain, N. E. *Energy Fuels* **2007**, *21*, 1042–1047.

(19) Schaub, T. M.; Hendrickson, C. L.; Qian, K. N.; Quinn, J. P.; Marshall, A. G. *Anal. Chem.* **2003**, *75*, 2172–2176.

(20) Schaub, T. M.; Rodgers, R. P.; Marshall, A. G. *Energy Fuels* **2005**, *19*, 1566–1573.

(21) Marshall, A. G.; Hendrickson, C. L.; Jackson, G. S. *Mass Spectrom. Rev.* **1998**, *17*, 1–35.

(22) Hughey, C. A.; Rodgers, R. P.; Marshall, A. G. *Anal. Chem.* **2002**, *74*, 4145–4149.

(23) Marshall, A. G.; Rodgers, R. P. *Acc. Chem. Res.* **2004**, *37*, 53–59.

(24) Rodgers, R. P.; Marshall, A. G. In *Asphaltenes, Heavy Oils and Petroleomics*; Mullins, O. C., Sheu, E. Y., Hammami, A., Marshall, A. G., Eds.; Springer: New York, 2007.

(25) Marshall, A. G.; Rodgers, R. P. *Proc. Natl. Acad. U.S.A.* **2008**, *105*, 18090–18095.

(26) McKenna, A. M.; Rodgers, R. P.; Purcell, J. M.; Smith, D. F.; Marshall, A. G. *Division of Petroleum Chemistry Symp. on Petrochemicals from Unconventional Fuels*, 236th Amer. Chem. Soc. Nat'l Mtg., Philadelphia, PA, August 17–21, 2008.

## Simulated Distillation of Middle Eastern Heavy Fractions

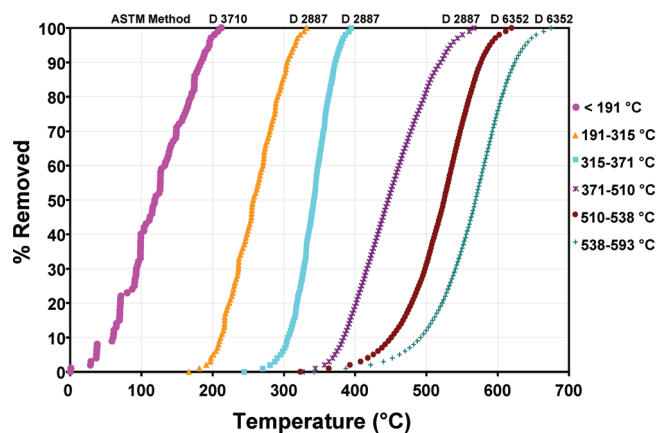


**Figure 1.** Compiled simulated distillation plots for six fractions showing the percentage removed as a function of temperature. The boiling range for each sample is obtained through gas chromatography (GC) distillation of a mixture of hydrocarbons with boiling points similar to the expected boiling range of the sample.

pot still: 191–315 °C, 315–371 °C, and  $\geq 371$  °C. The  $\geq 371$  °C material was further fractionated in a vacuum flash unit as follows. A prewarmed feed was trickled into a heated vessel held at  $\sim 2$  Torr to facilitate flash volatilization of material at an atmospheric equivalent temperature related to the vacuum and flash vessel temperature. Nonvolatilized materials were collected and then subjected to the flash operation at an increased temperature. Because this type of fractionation does not employ a column, separation is relatively poor, compared with a true fractional distillation. However, because the contact period at elevated temperature is short, yield is maximized with minimal coking and decomposition. This procedure afforded fractions with the atmospheric equivalent boiling point (AEBP), 371–510 °C, 510–538 °C, 538–593 °C, and the  $\geq 593$  °C “bottoms” remaining after collection of the 538–593 °C fraction. The results of simulated distillations performed in accordance with ASTM methods for each fraction are shown in Figure 1. Prior to APPI FT-ICR analysis,  $\sim 10$  mg from each fraction was diluted with 5 mL of toluene to make a stock solution, which was further diluted in toluene to yield a final concentration of 500  $\mu\text{g/mL}$  without additional modification.

**Instrumentation.** *APPI Source.* The APPI source (Thermo-Fisher Scientific, San Jose, CA) was coupled to the first pumping stage of a custom-built FT-ICR mass spectrometer (see below) through a custom-built interface.<sup>27,28</sup> A Hamilton gas-tight syringe (5 mL) and syringe pump were used to deliver the sample (50  $\mu\text{L}/\text{min}$ ) to the heated vaporizer region (250–375 °C)<sup>26</sup> of the APPI source, where  $\text{N}_2$  sheath gas (50 psi) facilitates nebulization, while the auxiliary port remained plugged. Gas-phase molecules flow out of the heated vaporizer in a confined jet and photoionization is initiated by a krypton vacuum ultraviolet gas discharge lamp (10 eV photons, 120 nm), where photoionization occurs. Toluene increases the ionization efficiency for nonpolar aromatic compounds by means of dopant-assisted APPI<sup>29,30</sup> through charge exchange, and proton transfer reactions occur between ionized toluene molecules and neutral analyte molecules at atmospheric pressure.<sup>27,29</sup> Protonated ions exhibit half-integer DBE values (DBE =  $c - h/2 + n/2 + 1$ , calculated from the ion elemental com-

position,  $\text{C}_c\text{H}_h\text{N}_n\text{O}_o\text{S}_s$ ) and may thus be distinguished from radical cations with integer DBE values.

**9.4 T FT-ICR MS.** Middle Eastern crude oil distillate fractions were analyzed with a custom-built FT-ICR mass spectrometer equipped with a 9.4 T horizontal 220 mm bore diameter superconducting solenoid magnet operated at room temperature (Oxford Corp., Oxney Mead, U.K.)<sup>31</sup> and a modular ICR data station (Predator) facilitated instrument control, data acquisition, and data analysis.<sup>32,33</sup> Positive ions generated at atmospheric pressure were accumulated in an external linear octopole ion trap<sup>34</sup> for 250–1000 ms and transferred by radio-frequency (rf)-only octopoles<sup>35</sup> to a 10-cm-diameter, 30-cm-long open cylindrical Penning ion trap. Octopoles were operated at 2.0 MHz and 240  $\text{V}_{\text{p-p}}$  amplitude. Broadband frequency sweep (chirp) dipolar excitation (70–700 kHz at 50  $\text{Hz}/\mu\text{s}$  sweep rate and 350  $\text{V}_{\text{p-p}}$  amplitude) was followed by direct-mode image current detection to yield 8 Mword time-domain data sets. Time-domain data sets were coadded (200–300 acquisitions), Hanning apodized, and zero-filled once before fast Fourier transform and magnitude calculation.<sup>36</sup>

**Broadband Phase Correction.** Because of the increased complexity at higher  $m/z$ , broadband phase correction was applied to the entire mass spectrum for the  $> 593$  °C fraction to increase resolution for isobaric species.<sup>37–41</sup> Briefly, Fourier transformation of discrete time-domain data yields real and imaginary frequency-domain spectra,  $\text{Re}(\omega)$  and  $\text{Im}(\omega)$ , which are linear combinations of absorption- and dispersion-mode components,  $A(\omega)$  and  $D(\omega)$ . Therefore FT-ICR spectra are conventionally displayed in magnitude (absolute-value) mode,  $M(\omega) = [(\text{Re}(\omega))^2 + (\text{Im}(\omega))^2]^{1/2}$ . As described in detail elsewhere,<sup>36</sup> it is possible to determine the phase angle,  $\varphi = \tan^{-1}[\text{Im}(\omega)/\text{Re}(\omega)]$ , for each peak, and then construct the appropriate linear combination of real and imaginary FT spectra to recover the absorption-mode display. Absorption-mode spectral resolving power is higher (by a factor of up to 2) than the magnitude-mode resolving power. Frequency-to- $m/z$  calibration and data analysis are subsequently performed as for magnitude-mode display.

**Mass Calibration and Data Analysis.** ICR frequencies were converted to ion masses based on the quadrupolar trapping potential approximation<sup>42,43</sup> and internally calibrated with

(31) Senko, M. W.; Hendrickson, C. L.; Pasa-Tolic, L.; Marto, J. A.; White, F. M.; Guan, S.; Marshall, A. G. *Rapid Commun. Mass Spectrom.* **1996**, *10*, 1824–1828.

(32) Senko, M. W.; Canterbury, J. D.; Guan, S.; Marshall, A. G. *Rapid Commun. Mass Spectrom.* **1996**, *10*, 1839–1844.

(33) Blakney, G. T.; van der Rest, G.; Johnson, J. R.; Freitas, M. A.; Drader, J. J.; Shi, S. D.-H.; Hendrickson, C. L.; Kelleher, N. L.; Marshall, A. G. In *Proceedings of the 49th American Society for Mass Spectrometry, Conference on Mass Spectrometry & Allied Topics*; American Society for Mass Spectrometry: Chicago, IL, 2001; p WPM265.

(34) Senko, M. W.; Hendrickson, C. L.; Emmett, M. R.; Shi, S. D.-H.; Marshall, A. G. *J. Am. Soc. Mass Spectrom.* **1997**, *8*, 970–976.

(35) Wilcox, B. E.; Hendrickson, C. L.; Marshall, A. G. *J. Am. Soc. Mass Spectrom.* **2002**, *13*, 1304–1312.

(36) Marshall, A. G.; Verdun, F. R. *Fourier Transforms in NMR, Optical, and Mass Spectrometry: A User's Handbook*; Elsevier: Amsterdam, 1990.

(37) Comisarow, M. B.; Marshall, A. G. *Can. J. Chem.* **1974**, *52*, 1997–1999.

(38) Marshall, A. G. *Chem. Phys. Lett.* **1979**, *63*, 515–518.

(39) Craig, E. C.; Santos, I.; Marshall, A. G. *Rapid Commun. Mass Spectrom.* **1987**, *1*, 33–37.

(40) Beu, S. C.; Blakney, G. T.; Quinn, J. P.; Hendrickson, C. L.; Marshall, A. G. *Anal. Chem.* **2004**, *76*, 5756–5761.

(41) Xian, F.; Hendrickson, C. L.; Blakney, G. T.; Beu, S. C.; Marshall, A. G. In *Proceedings of the 56th ASMS Conference on Mass Spectrometry & Allied Topics*, Denver, CO, June 1–5, 2008; Paper No. TP008.

(42) Ledford, E. B., Jr.; Rempel, D. L.; Gross, M. L. *Anal. Chem.* **1984**, *56*, 2744–2748.

(43) Shi, S. D.-H.; Drader, J. J.; Freitas, M. A.; Hendrickson, C. L.; Marshall, A. G. *Int. J. Mass Spectrom.* **2000**, *195/196*, 591–598.

(27) Purcell, J. M.; Hendrickson, C. L.; Rodgers, R. P.; Marshall, A. G. *Anal. Chem.* **2006**, *78*, 5906–5912.

(28) Purcell, J. M.; Hendrickson, C. L.; Rodgers, R. P.; Marshall, A. G. *J. Am. Soc. Mass Spectrom.* **2007**, *18*, 1682–1689.

(29) Robb, D. B.; Covey, T. R.; Bruins, A. P. *Anal. Chem.* **2000**, *72*, 3653–3659.

(30) Smith, D. F.; Robb, D. B.; Blades, M. W. *J. Am. Soc. Mass Spectrom.* **2009**, *20*, 73–79.

respect to a highly abundant homologous alkylation series differing in mass by integer multiples of 14.01565 Da (mass of a  $\text{CH}_2$  unit).<sup>44,45</sup> Experimentally measured masses were converted from the International Union of Pure and Applied Chemistry (IUPAC) mass scale to the Kendrick mass scale<sup>46</sup> to identify homologous series for each heteroatom class (i.e., species with the same  $\text{N}_x\text{O}_y\text{S}_z$  content, differing only by their degree of alkylation).<sup>23–25,44</sup> Peak assignments were performed by Kendrick mass defect analysis, as previously described.<sup>44</sup> For each elemental composition,  $\text{C}_c\text{H}_h\text{N}_n\text{O}_o\text{S}_s$ , the heteroatom class, type (double bond equivalents,  $\text{DBE} =$  the number of rings plus double bonds involving carbon)<sup>47</sup> and carbon number,  $c$ , were tabulated for subsequent generation of heteroatom class relative abundance distributions and graphical DBE vs carbon number images.

## Results and Discussion

**Simulated Distillation Behavior.** Each distillate and flash fraction was subjected to a simulated distillation, performed in accordance with an appropriate ASTM method (D3710 for  $<191$  °C; D2887 for 191–315 °C, 315–371 °C, and 371–510 °C; and D6352 for 510–538 °C and 538–593 °C). Briefly, each sample is introduced into a nonpolar open tubular gas chromatographic column to simulate its boiling point distribution. The column oven temperature is raised at a specific linear rate to effect separation of the hydrocarbon components in order of increasing boiling point. Boiling points are assigned to the time axis from a calibration curve obtained under the same chromatographic conditions through analysis of a known mixture of hydrocarbons that span the expected boiling range for each sample. The boiling point temperature at each reported percent removed (% removed) increment is calculated from the retention time calibration. Although the trend to higher boiling point with successive fractions is clear, the modest separation afforded by the flash unit is evident from the overlapping simulated boiling ranges for these heavy fractions (Figure 1).

**Elemental Composition Assignment.** Figure 2 shows a broadband positive-ion APPI FT-ICR mass spectrum of the 593<sup>+</sup> °C residual fraction for a Middle Eastern heavy crude oil. The achieved resolving power of 508 000 at  $m/z$  800 results in 26 896 mass spectral peaks, each with magnitude greater than  $6\sigma$  of the baseline rms noise ( $m/z$  500–1250) and mass distribution centered at  $m/z$  800 with  $\sim 91$  mass spectral peaks across a 1 Da segment. The time-domain signal duration was 5.6 s (Figure 2 inset) and the signal did not damp completely to zero during the acquisition period. All ions are singly charged, as evident from the unit  $m/z$  spacing between species differing by  $^{12}\text{C}_c$  vs  $^{13}\text{C}_1^{12}\text{C}_{c-1}$ . Due to the increased complexity associated with residual samples, such as the 593<sup>+</sup> °C fraction, we applied broadband phase correction to yield absorption-mode display with increased mass resolution, as described above.<sup>41</sup>

**Molecular Weight Distribution vs Boiling Point.** In Part 1 of this work, we correlated the Boduszynski model to the composition of middle distillates; therefore, we shall focus here on fractions boiling above 371 °C. As the distillation cut temperature increases, the center of the molecular weight distribution shifts to higher  $m/z$  values. Figure 3 shows the

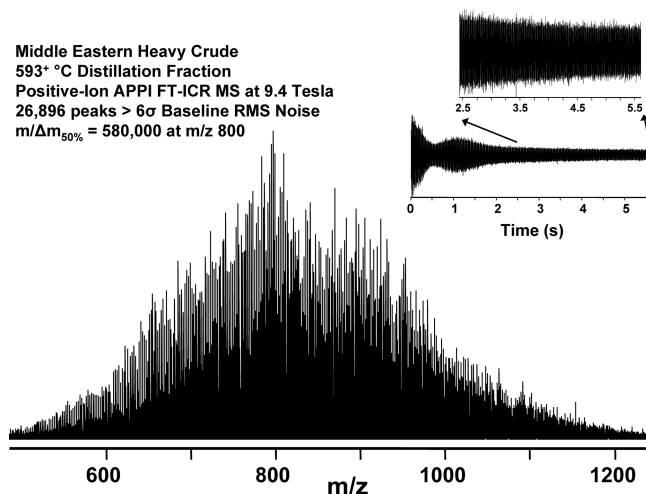


**Figure 2.** Broadband positive-ion APPI FT-ICR mass spectrum of a Middle Eastern heavy crude oil 593<sup>+</sup> °C distillate fraction. 26 896 mass spectral peaks were observed at 6 times the baseline rms noise, at an average mass resolving power,  $m/\Delta m_{50\%} = 580\,000$  at  $m/z$  800.

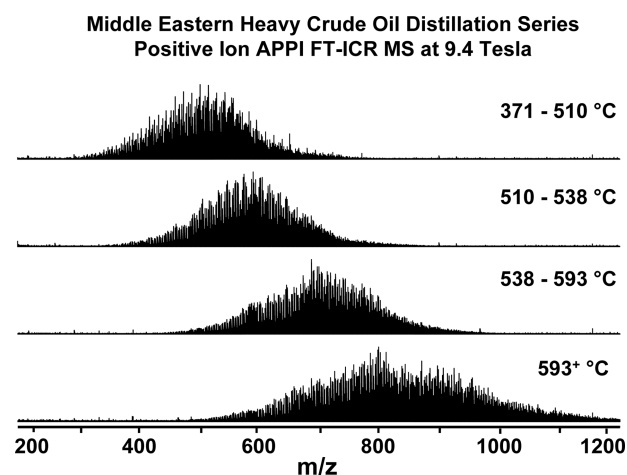


**Figure 3.** Broadband positive-ion APPI FT-ICR mass spectra for a full distillation series of Middle Eastern heavy crude oil. The molecular weight distribution broadens and shifts to higher mass with increasing boiling point.

broadband mass spectrum for four distillate fractions obtained from Middle Eastern heavy crude oil. The 371–510 °C fraction ranges from  $m/z$  300–800 with the mass distribution centered at  $m/z$  500 whereas the 593<sup>+</sup> °C fraction ranges from  $m/z$  500–1200, centered at  $m/z$  800. Although distillation limits the number of compound types and structure within each fraction, each distillation cut nevertheless contains many compound types, each comprised of a homologous alkylation series. Higher-boiling fractions contain higher-molecular-weight species and are more compositionally complex.<sup>1</sup> The mass distribution also broadens with increasing distillation temperature, because of the increasing number of possible compositions with increasing carbon number. Boduszynski outlined these two principles by application of field ionization and field desorption mass spectrometry to five distillation cuts and three sequential elution fractions from Boscan atmospheric residue; however, he lacked the resolving power to identify and characterize the species present in each fraction.<sup>1</sup>

**Heteroatom Class Distribution.** Figure 4 shows the heteroatom class distribution for all detected species of  $>1\%$

(44) Hughey, C. A.; Hendrickson, C. L.; Rodgers, R. P.; Marshall, A. G.; Qian, K. *Anal. Chem.* **2001**, *73*, 4676–4681.

(45) Qian, K.; Robbins, W. K.; Hughey, C. A.; Cooper, H. J.; Rodgers, R. P.; Marshall, A. G. *Energy Fuels* **2001**, *15*, 1505–1511.

(46) Kendrick, E. *Anal. Chem.* **1963**, *35*, 2146–2154.

(47) McLafferty, F. W.; Turecek, F. *Interpretation of Mass Spectra*; 4th ed.; University Science Books: Mill Valley, CA, 1993.

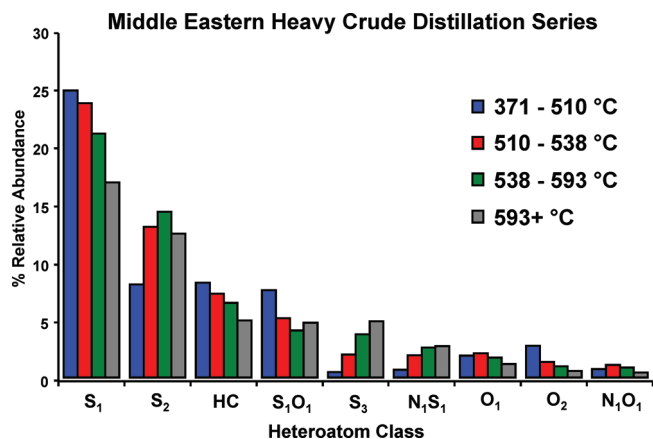


**Figure 4.** Heteroatom class distribution (heteroatom content) for Middle Eastern heavy crude oil distillation cuts and residue derived from positive-ion APPI FT-ICR MS. HC denotes molecules containing only hydrogen and carbon.

relative abundance in the APPI FT-ICR mass spectra for the three distillate fractions collected between 371 and 593 °C, as well as the  $\geq 593$  °C residuum from Middle Eastern heavy crude oil. Compounds containing a single S atom were the most abundant across the entire boiling range, followed by the S<sub>2</sub>, hydrocarbons, and SO classes. A decrease in the relative abundance of low heteroatom-containing compounds (e.g., hydrocarbons and S<sub>1</sub>) accompanies an increase in boiling point. Low molecular weight compounds are more volatile and therefore concentrate in lower-boiling fractions. A concurrent increase in the multiple-heteroatom classes (S<sub>1</sub> and S<sub>2</sub>) occurs as the boiling point increases. Multiheteroatomic species, such as S<sub>1</sub>O<sub>1</sub> and S<sub>2</sub>, have higher boiling points due to increased intermolecular attraction and are more abundant in higher distillate cuts as postulated in the Boduszynski model.<sup>1</sup> Weak dispersion forces dominate in alkanes and increase with alkyl chain length, with stronger intermolecular forces (e.g., hydrogen bonding,  $\pi$ - $\pi$  interactions) between aromatic rings systems and polar compounds.<sup>14</sup>

**Compositional Tests of the Boduszynski Hypothesis: DBE versus Carbon Number.** A plot of molar mass versus AEBP introduced by Boduszynski illustrates the correlation between the boiling point and molecular weight, structure, and heteroatom functionality in crude oil.<sup>1</sup> Briefly, for a given boiling point, saturated hydrocarbons have the highest molecular weight (carbon number), and condensed polyaromatic molecules, with several polar groups and little alkyl substitution, have the lowest molecular weight. Saturated hydrocarbons are problematic, because almost all ionization techniques result in extensive fragmentation, complicating the identification of neutral precursors. Therefore, we limit our comparison of APPI FT-ICR MS results with the Boduszynski model to compounds containing one or more cycloalkyl- or aromatic ring structures.<sup>48</sup> Careful examination of the molar mass versus AEBP shows that the incorporation of a single heteroatom to a hydrocarbon core structure results in a loss of  $\sim 2$ – $3$  C atoms per molecule to remain within the same boiling range. Compounds with multiple fused aromatic rings (higher DBE values) and polar functional groups (e.g., asphaltenes) have higher boiling points, because of stronger intermolecular forces, resulting in a lower

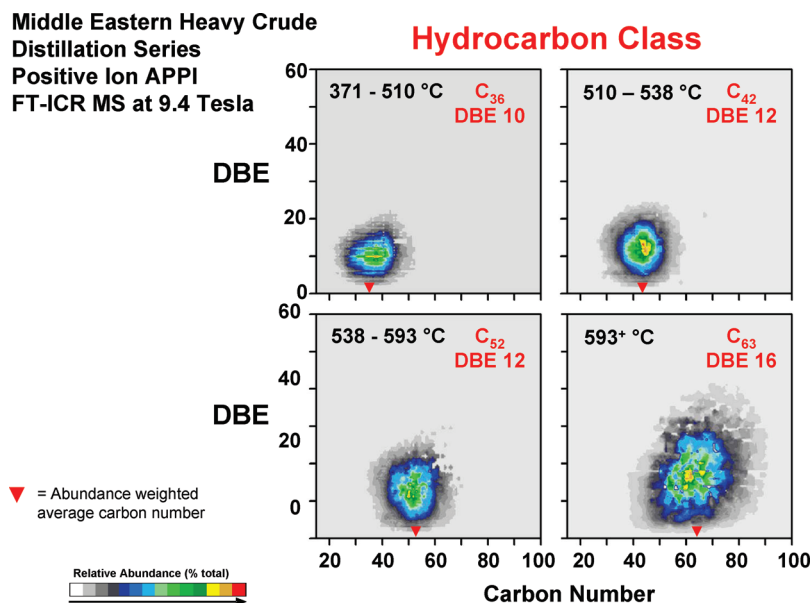
molar mass with higher aromaticity and heteroatom content.<sup>1</sup> Figure 5 shows isoabundance-contoured plots of DBE versus carbon number for the hydrocarbon class for three distillate fractions (371–510 °C, 510–538 °C, 538–593 °C, and  $\geq 593$  °C residue). Each subsequent flash fractionation is accompanied by an increase in the abundance-weighted average carbon number by  $\sim C_8$ – $C_{12}$  C atoms per structure, proceeding from C<sub>36</sub> in the 371–510 °C cut to C<sub>63</sub> in the residue. Aromaticity also increases with boiling point and is indicated by an increase in abundance-weighted DBE from 10 to 16 across the boiling range. The Boduszynski model postulates that hydrocarbons have the highest molar mass within a given boiling point. An increase in the number of heteroatoms and aromatic structures per molecule results in a shift to lower carbon number to remain at a given boiling point and results in a lower molecular weight for heteroatom-containing compounds. Heavy crude oils, such as the Middle Eastern heavy crude employed in this work, are rich in sulfur-containing species. Therefore, a comparison of the DBE and carbon number distributions for the hydrocarbon, S<sub>1</sub>, and S<sub>2</sub> classes serves to test the Boduszynski model, based on ultrahigh-resolution FT-ICR MS data.

Figure 6 shows DBE versus carbon number plots for the S<sub>1</sub> class for the same four distillate fractions. A similar trend is observed for the hydrocarbon class, but beginning at lower carbon number and DBE values for each boiling range, because of the incorporation of a sulfur atom into the molecular structure. The average molecular weight increases steadily with increasing boiling point from C<sub>35</sub> for the 371–510 °C cut to C<sub>59</sub> for the  $\geq 593$  °C residue. DBE values also increase from 9 to 14 across the boiling point range. If we compare the carbon number of highest relative abundance for each distillation cut for the hydrocarbon class and the S<sub>1</sub> class, we see a trend similar to that proposed by the Boduszynski model. For example, the hydrocarbon class for the 371–510 °C cut has a carbon number distribution between C<sub>22</sub>–C<sub>52</sub> with the highest abundance at C<sub>38</sub>. Within the same boiling point range, the addition of a S atom shifts the carbon number distribution to C<sub>20</sub>–C<sub>50</sub> with the highest abundance of C atoms per molecule at C<sub>35</sub>. The other fractions exhibit similar behavior, with less noticeable shifts for the residue fraction, because it is not a “true” distillation cut with a defined upper boiling point.

Compositional trends are further illustrated by DBE versus carbon number images for the S<sub>2</sub> class (Figure 7). The average carbon number increases across the series from C<sub>35</sub> to C<sub>56</sub> with an increase in DBE from 9 to 16. Approximately 2–4 fewer C atoms per molecule are associated with the addition of each heteroatom class, in agreement with the  $\sim 2$ – $3$  C atom decrease predicted by Boduszynski.

**The Compositional Continuum for Heavy Distillates.** To further corroborate the idea of continuity in composition and boiling point across the entire boiling range, a single combined plot of DBE versus carbon number for the S<sub>1</sub> class for all four heavy fractions is shown in Figure 8. Relative abundances for each spectrum are normalized separately for each boiling point range, and all individually scaled mass spectra are combined into a single DBE versus carbon number image. The gradual progression to higher carbon number (molecular weight) and DBE (aromaticity and hydrogen deficiency) extends from the 371–510 °C fraction to the 593<sup>+</sup> °C residue. A gradual increase in carbon number from  $\sim C_{25}$  to C<sub>90</sub> across the high boiling fractions is accompanied by an increase in aromaticity from DBE  $\approx 2$  to DBE  $\approx 40$ , an average of  $\sim 6$ – $8$  aromatic rings, which suggests that the

(48) Rodgers, R. P.; Marshall, A. G. *Proc. Natl. Acad. Sci. U.S.A.* 2008, 105, 1–6.



**Figure 5.** Isoabundance-contoured plots of double bond equivalents (DBE) versus carbon number for the hydrocarbon class of a Middle Eastern heavy crude oil distillation series and residue.

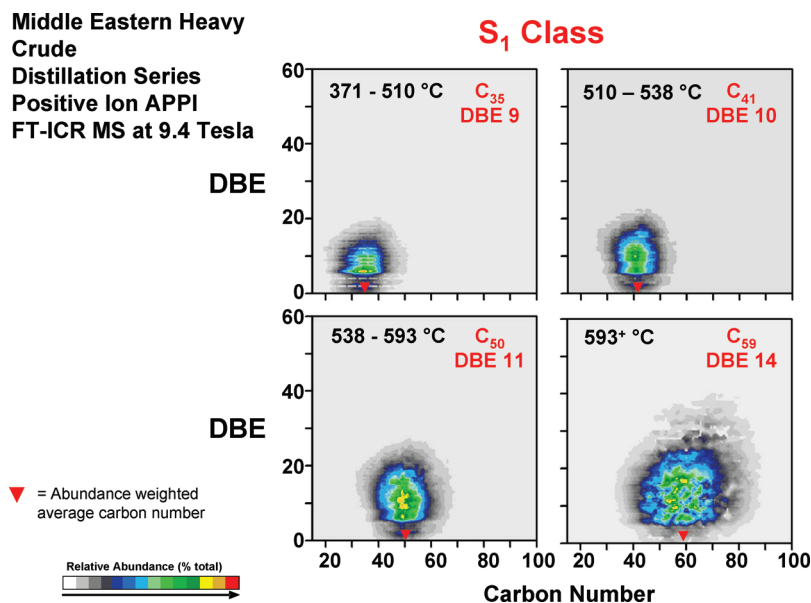


**Figure 6.** DBE versus carbon number for the S<sub>1</sub> class of a Middle Eastern heavy crude oil distillation series and residue.

crude oil composition varies continuously in both carbon number and DBE across the entire distillation range.

Figure 9 shows the same continuity trend in DBE and carbon number for the S<sub>2</sub> class in a single composite isoabundance-contoured plot for the entire distillation series. A similar trend is observed for the S<sub>1</sub> class, further supporting the proposed continuum model of crude oil.

**Implications for Asphaltene (Nondistillable) Composition.** The first successful, detailed compositional analysis of HVGO (Part I) and *distillable* heavy petroleum species up to the limit of distillation provides a unique opportunity to evaluate the compositional continuum of *nondistillable* materials, such as asphaltenes. With regard to the controversy as to whether asphaltenes are high-molecular-weight (> 4000 Da) or low-molecular-weight (400–2000) species, the scientific community uniformly agrees on asphaltene bulk elemental measurements (H:C ≈ 1). On one side, the high molecular weight of

asphaltenes is believed to account for its high heteroatom content, insolubility in *n*-alkanes, self-association, nondistillable nature, and deposition tendencies. However, if correct, the continuity model (here, proved accurate for all distillable petroleum materials) requires “high molecular weight” asphaltenes (nondistillables) to follow distillable compositional trends (e.g., growth in aromaticity with increased carbon number). That assertion is now testable. Because the high mass accuracy afforded by FT-ICR mass spectrometry provides the elemental compositions for all mass spectral species, it is possible to track the hydrogen-to-carbon (H:C) atomic ratio of all species, as a function of increased boiling point. Class-dependent compositional trends allow for extrapolation into the proposed “high molecular weight” nondistillable compositional space. Simply, *if* nondistillables constitute a linear extension from distillable compositional space with the requisite increase in carbon number and aromaticity, it is

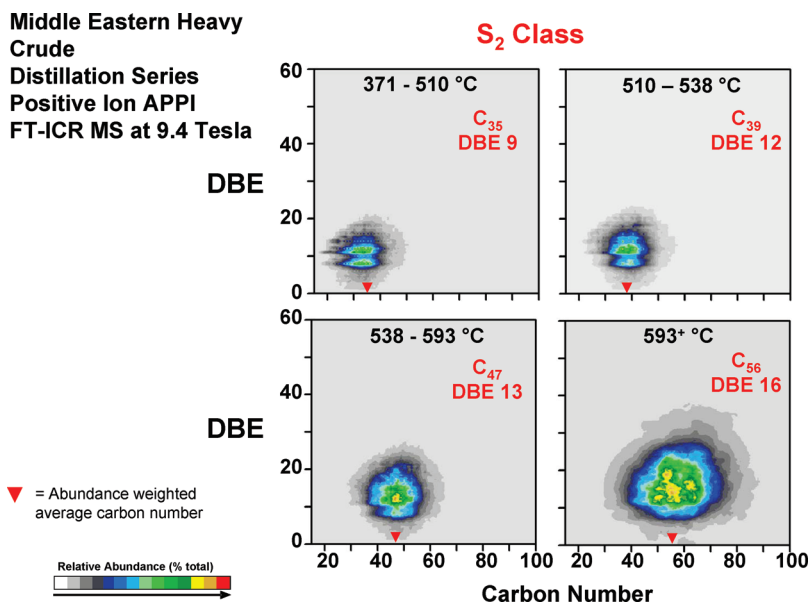


Figure 7. DBE versus carbon number for the S<sub>2</sub> class of a Middle Eastern heavy crude oil distillation series and residue.

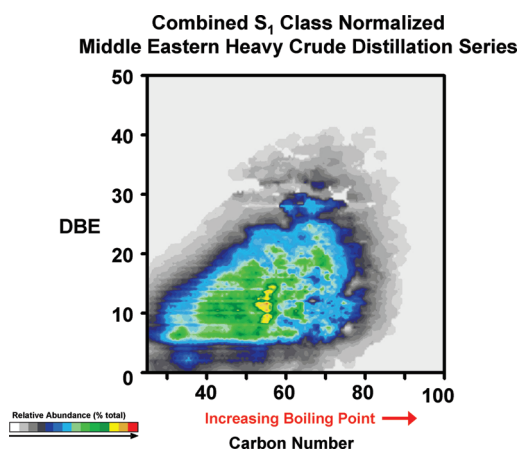


Figure 8. Composite isoabundance contoured plot of DBE vs carbon number for the combined S<sub>1</sub> class for Middle Eastern heavy crude oil distillation series and residue. The mass spectrum for each boiling point is normalized separately to illustrate the global continuum in carbon number and DBE, as a function of increasing boiling point.

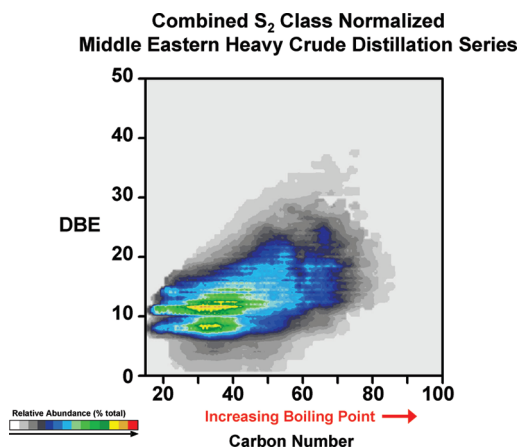


Figure 9. Composite isoabundance contoured plot of DBE versus carbon number, as in Figure 8, but for the combined S<sub>2</sub> class for Middle Eastern heavy crude oil distillation series and residue.

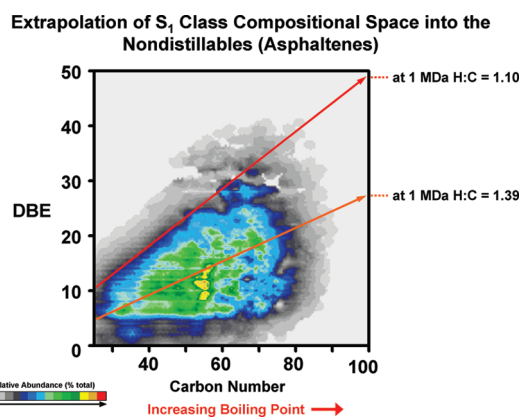


Figure 10. Composite isoabundance contoured plot of DBE versus carbon number for the S<sub>1</sub> class for Middle Eastern heavy crude oil distillation series and residue. (See text for extrapolations to higher carbon numbers.)

possible to predict nondistillable (asphaltene) molecular weight from a comparison of tens of thousands of individual species with, ironically, bulk H:C ratios.

Figure 10 was compiled from all S<sub>1</sub> class species identified from the distillation cuts. An abundance-weighted average trend line (orange) has been added to facilitate conversion of carbon number and DBE to elemental H:C ratios for the S class components. Extension of that line beyond distillable space and into nondistillable (asphaltene) space results in an inadequate decrease in the H:C ratio as the carbon number increases. As a consequence, extrapolation of the entire continuum compositional space (> 110 000 elemental compositions in this study) to higher carbon numbers cannot account for asphaltenes. Hence, the seeds of the petroleum compositional continuum are planted in the lowest boiling fractions and progress continuously as the carbon number increases. To evaluate the decrease in abundance weighted H:C ratio as a function of increased carbon number, one can project the trend line to extremely high carbon numbers. Surprisingly, projection of the trend line beyond 1 MDa leads to an H:C ratio of only 1.39, far greater than the accepted bulk H:C ratio for asphaltenes. Furthermore,

projection of the lowest H:C ratio (most aromatic) upper boundary of distillable compositional space (red line) to 1 MDa yields an H:C = 1.1, which is more similar to that for asphaltenes but is orders of magnitude greater in molecular weight than even the heaviest proposed asphaltenes. Thus, linear extrapolation of the distillable compositional space to *higher carbon number* cannot account for the asphaltene (nondistillable) composition. Within the scope of the *continuity* model, the proposed existence of high-molecular-weight (> 2000 Da) nondistillables presents a paradox. To account for the low bulk H:C ratio of asphaltenes, there would have to be a *discontinuity* in compositional space. Analysis of other compositional classes with similar and increased heteroatom content yielded similar results. In parts 3–5 of this 5-part series, we shall systematically address the application and success of extending the continuity model to describe nondistillable fractions.

### Conclusions

Here, we present evidence that supports the descriptive model proposed by Boduszynski and others: crude oil is a continuum in molecular weight, structure, and boiling point. Employing ultrahigh-resolution FT-ICR MS of heavy crude oil over the past two decades, we are able to provide data that strongly support this continuity model through comparisons of the molecular weight distribution, DBE, and carbon

number for a Middle Eastern heavy crude oil. Previous work supported this model for middle distillate fractions (HVGO) from an unconventional crude.<sup>26</sup> Here, we correlate a full distillation series for a single whole conventional crude oil to the Boduszynski model. For all tested heteroatom classes, the class-defined compositional space grows in carbon number and aromaticity (DBE) in agreement with the continuity model. However, projection of distillable compositional space to higher carbon number cannot accurately describe nondistillables due to incompatibility with bulk asphaltene H:C ratios. The inescapable conclusion is that either asphaltenes (nondistillables) are not high molecular weight species, or the continuity model is not applicable to nondistillable materials.

**Acknowledgment.** The authors thank John P. Quinn for maintenance of the 9.4 T instrument and Christopher L. Hendrickson for help in optimization of instrument parameters. This work was supported by NSF Division of Materials Research (through DMR-0654118) and the State of Florida, Florida State University, and the National High Magnetic Field Laboratory in Tallahassee, FL. The authors also thank Shell Global Solutions, Houston, TX, for financial support.

**Note Added after ASAP Publication.** The text was modified in the version of this paper published ASAP May 3, 2010; the corrected version published ASAP May 6, 2010.